Autoionization of Ba $6p_{1/2}nk$ states in static and microwave fields below the Inglis-Teller limit

R. R. Jones and T. F. Gallagher
Department of Physics, University of Virginia, Charlottesville, Virginia 22901
(Received 17 October 1988)

Measurements of the autoionization rates of $6p_{1/2}nk$ states of Ba in the presence of static and 9-GHz microwave fields have been performed using a multistep laser excitation technique. For field amplitudes below $1/3n^5$, which defines the Inglis-Teller limit, the measured rates in both static and dynamic fields are in good agreement with a simple Stark-effect model. The rates show an n^{-4} scaling rather than the familiar n^{-3} dependence observed in zero field. We also report the first observation of forced autoionization by microwaves. Connections between our measurements and the physical situation in plasmas are discussed, including implications for dielectronic recombination.

INTRODUCTION

When considering dielectronic recombination of impurity ions in a plasma, we must take into account the other effects on the impurity ions due to the large number of electrons and the positive ions, mostly hydrogen, present in the plasma. Since the electrons move much more rapidly than the ions, their effect is usually described in terms of collision processes.[1] The effect of the ions, which move slowly, is often described in terms of a static electric field,[2] the assumption being that the temporal fluctuations of the ionic electric fields are slower than processes of interest. Using such a model Jacobs *et al.*[1,2] have predicted that these microscopic electric fields can substantially increase the dielectronic recombination rate. The origin of this increase in rate is easily understood using the hydrogenic model of Jacobs *et al.*,[1,2] which is strictly valid to the Inglis-Teller limit, defined by $E=1/3n^5$. The Inglis-Teller limit is the point at which the members of a series are no longer spectrally resolved. The origin of the relation $E=1/3n^5$ is as follows. The energy spacing between the n and $n+1$ levels is $1/n^3$, and the Stark shifts of the highest and lowest energy $|m|=0$ Stark states of principal quantum number n are $\pm 3n^2E/2$. Thus when $E=1/3n^5$ the extreme Stark status of principal quantum numbers n and $n+1$ overlap, producing a nearly continuous distribution of levels. In a field the good hydrogenic quantum states are the Stark states, with quantum numbers n,k,m instead of n,l,m and there exists a linear, field-independent transformation between the two sets of states with transformation matrix elements given by Wigner 3-J symbols.[3] Each of the nkm states has some character from each of the allowed nlm states, $|m|\leq l\leq n-1$. As a result, each of the l states is spread over the entire Stark manifold, leading to an essentially continuous absorption spectrum from a low-lying state. In addition, since the autoionization rates fall rapidly with increasing l,[4] the overall effect is to redistribute the rapid autoionization rates of the lowest l states over the Stark states. The total recombination rate for a given n can be written as

$$A_{\mathrm{DR}}(n)=\sum_l \beta\frac{A_A(l)A_R(l)}{A_A(l)+A_R(l)}\ ,$$

where $A_A(l)$ and $A_R(l)$ are the autoionization and radiative decay rates for a given l state and β is a constant. In the lower l, lower n states $A_A \gg A_R$, so much of the autoionization rate can be shared without any dimunition of the recombination rate.[5] Therefore the net result is an increase in the overall rate because the high-angular-momentum states, which previously did not contribute to the dielectronic recombination rate, have been converted to Stark states which do. The validity of the theory of Jacobs *et al.*[1,2] has been verified by the recent crossed-beam dielectronic recombination experiments of Dunn *et al.*[3] in which small static electric fields have been shown to dramatically alter the dielectronic recombination rates.[5,6]

One of the assumptions made in treating the ion microfields is that they are static, or at least slowly varying, on the time scale of the processes of interest. However this is not necessarily the case. As we have shown recently, the autoionization rates of Ba $6pnl$ states decrease very rapidly with increasing l. For $n=11$ the highest-angular-momentum states have autoionization rates below the radiative decay rate of 10^8 s^{-1}.[4,7] If we consider a plasma of electron or singly charged ion density ρ and a temperature T, the thermal motion of the ions generates fields which fluctuate at frequencies $\sim v_T\rho^{1/3}$, where v_T is the mean thermal velocity $(kT/2m)^{1/2}$. For $\rho=10^{15}$ cm^{-3} and $T=10^4$ K this frequency is $\sim 10^{11}$ Hz, far in excess of the autoionization rates of the highest l states. Apparently in a real plasma the initial assumption of slowly varying ion microfields is not met.

To explore the effect of rapid time variations we have measured autoionization rates of Ba $6pnk$ states in static and 9.25-GHz microwave electric fields, which provide a reasonable approximation to the time varying microfields in a plasma. In the sections that follow we describe our experimental approach, present the results, and discuss the implications for dielectronic recombination.

EXPERIMENTAL APPROACH

We use a multistep laser excitation scheme, shown in Fig. 1, to excite Ba atoms from the $6s^2\,{}^1S_0$ ground state to a $6pnk$ autoionizing state in the presence of static or microwave fields using three tunable dye lasers.[8,9] This process is precisely the inverse of the dielectronic recombination mechanism which has been described previously. The first two Hansch[10] dye lasers excite the ground-state atoms through the Ba $6s6p\,{}^1P_1$ state to a $6snl$ Rydberg level. The atomic system is now well described as a single electron in a Coulomb orbit about a positively charged core. The final laser excitation to the $6pnl$ autoionizing state is achieved by driving the Ba^+ core $6s$-$6p$ transition. This is the strong Ba^+ resonance line whose transition probability is several orders of magnitude larger than direct continuum excitation of the outer Rydberg electron.[8,9] Thus the Rydberg electron remains a spectator throughout the process, and we observe transitions to the bound autoionizing state only, with no direct continuum excitation.

The first dye laser is pumped by the second harmonic of a Nd:YAG laser at 532 nm and is used to excite the Ba $6s6p\,{}^1P_1$ state at 18060 cm^{-1} as shown in Fig. 2. The second dye-laser pulse excites Ba atoms from the $6s6p$ state to a $6snl$ Rydberg state and is pumped by the Nd:YAG third harmonic at 355 nm. Both of these lasers have linewidths of approximately 1 cm^{-1} and temporal widths of 10 ns. The second dye-laser pulse is delayed by 5 ns after the first laser to ensure saturation of the $6s^2$-$6s6p$ transition before the arrival of the second laser pulse. The third dye laser, which is used to drive the Ba^+ $6s$-$6p$ ion line, is pumped by an excimer laser operating with XeCl at 308 nm. This dye laser has a linewidth of 0.3 cm^{-1} and a pulse length of 10 ns. All three dye lasers are linearly polarized in the same direction, are pulsed at 20 Hz, and have pulse energies on the order of 100 μJ.

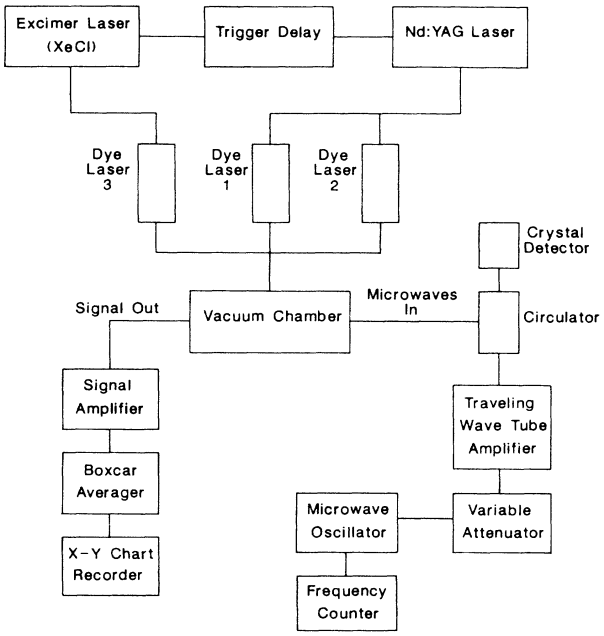

FIG. 2. Simple diagram of the experimental apparatus showing the dye laser, microwave, and detection equipment.

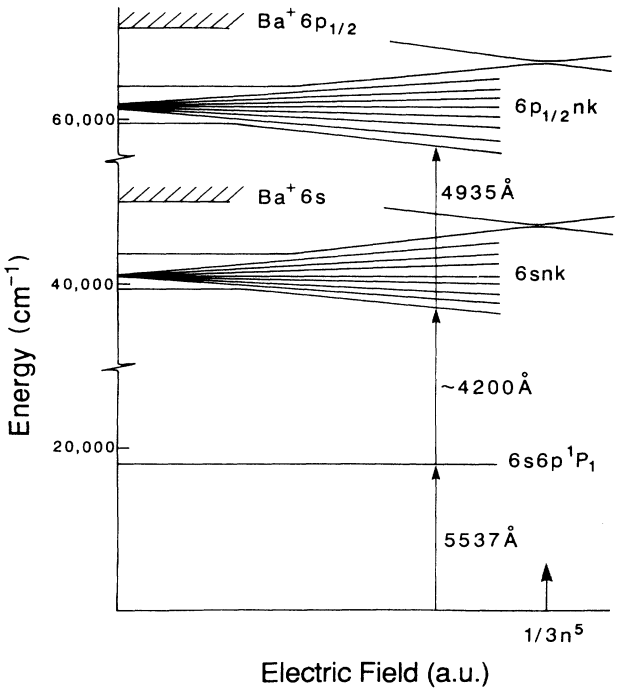

FIG. 1. Excitation diagram of Ba $6p_{1/2}nk$ autoionizing states in nonzero fields. This figure (not drawn to scale) shows the stepwise excitation of the autoionizing level via the $6s6p\,{}^1P_1$ resonance line and $6snk$ Stark states.

The Ba atoms are excited in an effusive beam originating from a resistively heated oven in a vacuum chamber with a background pressure of 10^{-6} Torr. The Ba atoms interact with the three laser beams approximately 15 cm from the oven inside a microwave cavity as shown in Fig. 3. The cavity consists of a 20-cm-long section of X-band WR90 rectangular waveguide with flanges on both ends. Two holes of 0.125-cm diameter are centered on opposite sides of the cavity in order to allow the atomic and laser beams to interact colinearly in the cavity center. A thin copper septum placed in the vertical center of the cavity allows atoms in the interaction region to be exposed to dc or ramping fields as well as microwaves. The plate separation between the septum and the upper wall of the cavity is 0.47 cm.

After the laser excitation the excited atoms autoionize and a small voltage is applied to the septum which pushes the Ba^+ ions (or electrons) through a 0.10-cm diameter hole centered in the top of the cavity toward a dual microchannel plate detecter which is located approximately 10 cm above the cavity. The signal from the microchannel plates is directed through a signal amplifier and a boxcar averager before being recorded on an X-Y chart recorder.

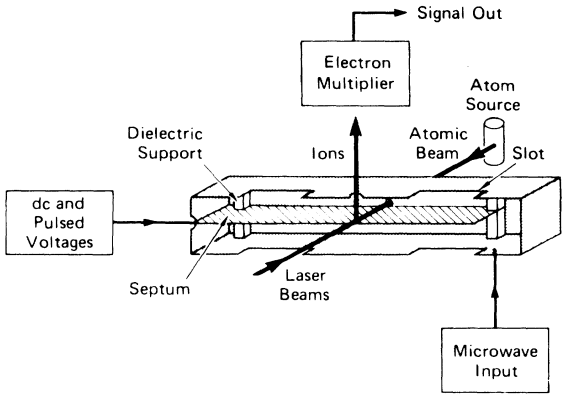

FIG. 3. Schematic of the interaction region in the vacuum chamber. The three dye-laser beams interact with the atomic beam inside a microwave cavity. After autoionization the Ba^+ ions are pushed toward the detection region by applying a voltage to the septum.

For static field measurements, all three dye lasers are fired in dc fields which range from zero up to the classical ionization limit of $1/16n^4$, where n is the effective quantum number of the Rydberg state. The static fields are produced by simply applying a constant voltage to the septum in the cavity.

Our microwave source is a variable frequency oscillator which is tunable from 8–12 GHz. The oscillator is tuned to excite the TE_{109} mode of the microwave cavity at 9.25 GHz which has an antinode at the position of the extraction aperture. The microwave frequency is kept at the cavity resonance by constantly monitoring the reflected power from the cavity with a crystal detector and also by observing the oscillator output with a frequency counter. The microwaves are amplified by a traveling wave tube amplifier before being coupled to the cavity through a probe one-quarter wavelength from one end of the cavity. Fields of up to 2500 V/cm can be reached in the cavity which has a resonant frequency to bandwidth ratio $Q=1025$. The field strength in the cavity is ajdusted using a variable attenuator located between the oscillator and the TWT amplifier. Since microwave fields ionize Ba Rydberg levels at fields greater than $0.28/n^5$,[11] rather than $1/16n^4$, measurements in microwave fields are only done in fields less than $0.28/n^5$.

EXPERIMENTAL RESULTS

Autoionization of the $6p_{1/2}nk$ levels in static and microwave fields

The autoionization rates and energies of the $6p_{1/2}nk$ levels are determined by scanning the third laser frequency over the autoionizing resonance near the Ba^+ $6s$-$6p$ transition. The power of the third laser is maintained at a level such that the ion signal amplitude is a linear function of laser power. In this way we prevent depletion broadening[12] of the resonance, and the autoionization rate can be taken as the FWHM of the observed Lorentzian profile.

Scans of the third laser frequency have been performed for a series of states with effective quantum numbers between 15 and 20. The changes in the autoionization widths and profile positions and shapes are observed, for a constant effective quantum number, as the static or microwave field amplitude was increased from zero to $0.28/n^5$. For these scans the second laser is tuned so as to excite the zero field s or d states, and the third laser is fired within 10 ns after the second laser and in the presence of the field. Typical scans for levels with effective quantum number $n=15.3$ at various microwave powers are shown in Fig. 4. Similar scans in static fields are shown in Fig. 5. Figures 4 and 5 clearly show the change in the composition of the wave function of the energy level studied with changing field. In zero field the profile is the simple Lorentzian profile of the $6p_{1/2}18d$ state. With increasing field, character of the nearby p state is gradually mixed into the $18d$ level and eventually becomes dominant. At fields $\sim 1.3n^5$ the original $18d$ state becomes a

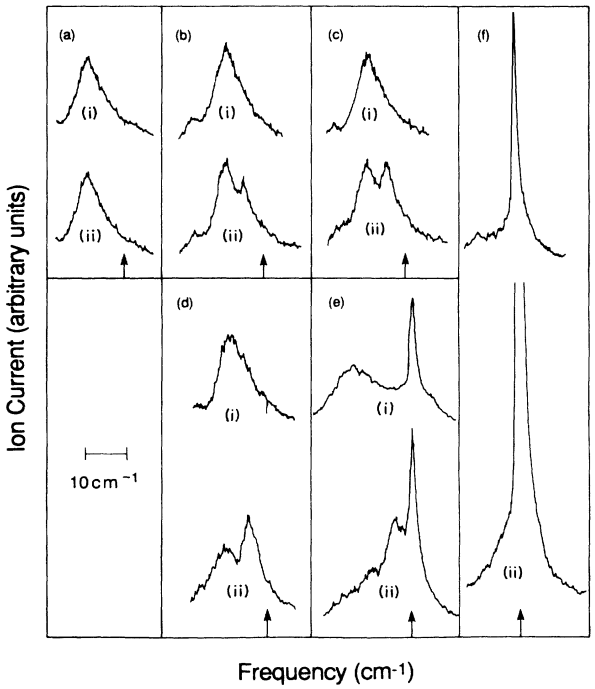

FIG. 4. Frequency scans of the third dye laser showing the evolution of the $6p_{1/2}nk$ autoionizing state which has an initial Rydberg state with effective quantum number 15.3. Scans were taken with the third laser appearing after (i) and before (ii) the microwaves were removed from the cavity. Field values shown are (a) 0 V/cm, (b) 140 V/cm, (c) 260 V/cm, (d) 475 V/cm, (e) 875 V/cm, and (f) 1635 V/cm. The Inglis-Teller limit occurs at $n=15$ for $E=2.26$ kV/cm. The fields used in (a)–(f) correspond, respectively, to 0%, 6%, 11%, 21%, 39%, and 72% of this field. Arrows mark the Ba^+ $6s$-$6p_{1/2}$ ion transition at 20 261.6 cm^{-1} and the frequency scale for all scans is shown in the lower left.

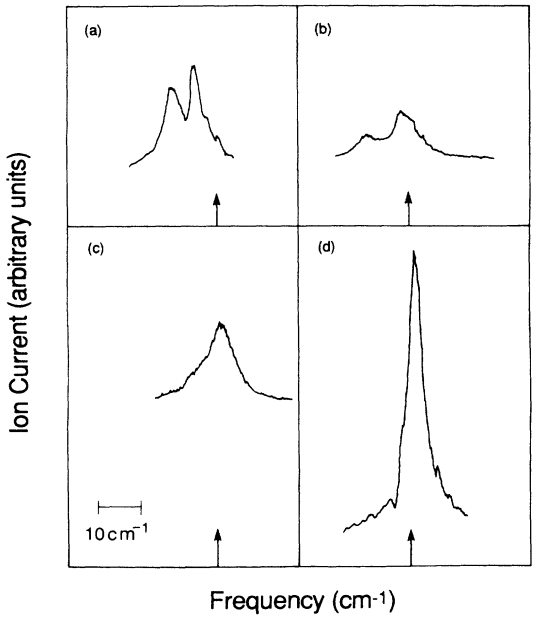

FIG. 5. Frequency scans over the same autoionizing states shown in Fig. 4, but in static instead of microwave fields. Fields displayed are (a) 200 V/cm, (b) 500 V/cm, (c) 1000 V/cm, and (d) 2000 V/cm. The Inglis-Teller limit occurs at $n=15$ for a field of 2.26 kV/cm. The fields used in (a)–(d) correspond, respectively, to 9%, 22%, 44%, and 89% of this field. Arrows mark the ion transition line at 20 261.6 cm^{-1} and the scale for the scans is shown in the lower left.

mixture of high-angular-momentum levels which leads to a very sharp resonance at, or very near, the ion transition.

Also shown for comparison in Fig. 4 are frequency scans of the third laser when its temporal position has been delayed until after the microwaves have been turned off in the cavity, allowing the $6snk$ atoms to relax to one or many zero field $6snl$ states. As shown in Figs. 4(b)–4(d) the major difference between having the microwaves on or off is that when they are turned off the second component corresponding to the $6s19p \rightarrow 6p19p$ excitation disappears. Note that up to the field corresponding to Fig. 4(f) most of the excitation strength is concentrated in the $18d$ or $19p$ resonances, with very little in the feature at the ion transition frequency. Only at the field of Fig. 4(f) are the d and p states well mixed with the high-angular-momentum states of the Stark manifold. Therefore at fields less than $1/3n^5$, neither p nor d character is well mixed into the manifold. Furthermore, if the inner manifold states contain no p or d character, then they will not interact with s levels. Thus, if these simple arguments hold, only angular momentum values with $l>3$ are well mixed in the manifold for microwave field amplitudes, $E>1/3n^5$. We will discuss some implications of this observation in proceeding sections.

The excitation profiles of autoionizing resonances in dc fields exhibit a wide variety of widths and shapes for fields between $1/3n^5$ and $1/16n^4$. The origin of the variation is easily understood. In this field regime the Stark manifolds of several different principle quantum numbers overlap, and there are many avoided level crossings between states of different n. Near these avoided level crossings the wave function composition of the interacting levels changes drastically. Thus, it is expected that the autoionization rates should show wild variations with changing field or effective quantum number. Scans of the third laser frequency at static fields which are 80% of the classical ionization field ($E=1/16n^4$) were taken for a range of effective quantum numbers between 15 and 20. The excitation profiles exhibited varying widths and often multiple peaks instead of the characteristic single Lorentzian profile with widths scaling as n^{-3}. In addition, studies of the $6p_{1/2}nk$ states for n between 13 and 20 have been performed in dc fields of 80% of the microwave ionization limit. The average widths (FWHM) of the observed features of the resonances are shown in Fig. 6(a). The values plotted in Fig. 6(a) are obtained by deconvoluting the Gaussian width of the laser line from the observed Voight profiles. Measurements have also been carried out in microwave fields from 70% to 100% of the microwave ionization field of $0.28/n^5$. For these studies the third laser pulse has been delayed after the second laser pulse by 10–1000 ns in an attempt to observe any time dependence of the state mixings. However, the third laser frequency scans are unaffected by this variation in temporal separation between the last two laser pulses. For measurements made in microwave fields of $0.28/n^5$, electron current is measured rather than ion current. This procedure allows us to time resolve the autoionization signal from the microwave ionization signal. In all cases the profiles observed are sharp resonances at the Ba^+ $6s_{1/2}-6p_{1/2}$ transition, and the FWHM of the Lorentzian resonances are obtained by deconvoluting the Gaussian laser line from the observed Voigt profile. Observed autoionization widths in the microwave fields are plotted in Fig. 6(b), which shows a clear n^{-4} scaling.

The autoionization rates $A_A(nk)$ of Fig. 6 can be fit to n^{-4} scalings with the following results. For static fields

$$A_A(nk)=6.7\times10^4 n^{-4}(\mathrm{cm}^{-1})$$
$$=0.31n^{-4}(\mathrm{a.u.})$$

and for microwaves

$$A_A(nk)=5.4\times10^4 n^{-4}(\mathrm{cm}^{-1})$$
$$=0.25n^{-4}(\mathrm{a.u.})\,.$$

It is somewhat ironic that the microwave-field data of Fig. 6(b) exhibit such a clear n^{-4} scaling. At the outset it was by no means apparent that we would find such a simple result. To understand the n^{-4} scaling in both these cases we consider the Stark-effect model first used by Jaffe *et al.*[13] We begin with the static field case. In the approximation that all the $6pnk$ Stark states of $m=0$ have the same autoionization rate, the rate is given by the mean of the values of the autoionization rates of the $6pnl$ states, $A_A(nl)$, i.e.,

$$A_A(nk)=\sum_{l=0}^{n-1}\frac{A_A(nl)}{n} . \quad (1)$$

From the l dependence discussed previously, it is clear that the low l states have vastly higher autoionization rates than the high l states. Thus a Stark state, which is a mixture of l states, has an autoionization rate that reflects the amount of low l character. For the $m=0$ states, 95% of the total autoionization rate is derived from the states of $l \leq 4$.

We can take advantage of the dominance of the low l autoionization rates to define the total scaled autoionization rate $A_A(m)$ which is independent of n. Specifically, for $m=0$,

$$\frac{A_A(0)}{n^3}=\sum_{l=0}^{n-1}A_A(nl) . \quad (2)$$

Using Eq. (2) we can rewrite Eq. (1) as

$$A_A(nk)=\frac{A_A(0)}{n^4} . \quad (3)$$

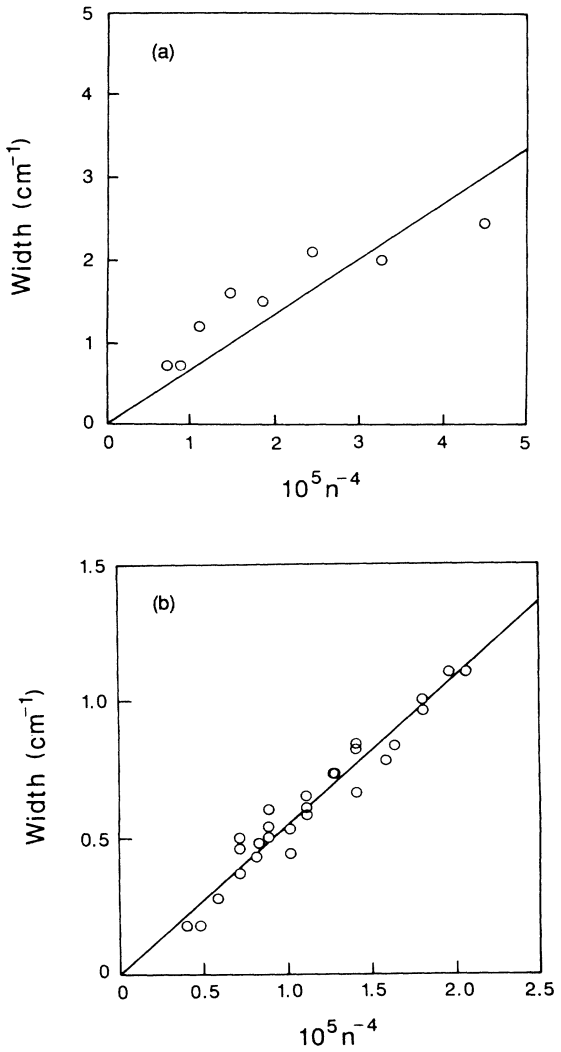

FIG. 6. (a) Plot of autoionization rates measured in static fields of $0.21/n^5$ vs n^{-4}. The best linear fit shown has a slope of 6.7×10^4 cm^{-1} and the uncertainties in the data are 0.05 cm^{-1}. (b) Plot of autoionization rates measured in microwave fields vs n^{-4}. Data were taken in microwave fields of $0.21/n^5$ and $0.28/n^5$ (the Ba microwave ionization limit). Measurements shown were taken with the third laser firing in the presence of the microwaves and delayed by 10–500 ns after the second laser. Uncertainties in the data points are 0.05 cm^{-1}. The best linear fit shown has a slope of $5.4\times10^4 n^{-4}$ cm^{-1}.

Fortunately, the autoionization rates of the Ba $6pnl$ states have been measured previously by various authors.[4,14,17] The scaled rates, $n^3\Gamma$, are listed in Table I. Using the rates from Table I and Eq. (3) we obtain $A_A(nk)=0.53n^{-4}$ in atomic units. Considering the simplicity of our model, this value is in relatively good agreement with our static field measurements and with those reported previously by Safinya *et al.*[18]

Although this simple model seems pefectly reasonable for static fields, the fact that single, sharp resonances are observed in microwave fields is somewhat surprising. If we think of the Stark effect in quasistatic terms, an $n=20$ atom in a microwave field of 1 kV/cm undergoes energy variations over a wide range of as much as ±24 cm^{-1} during each microwave cycle, and we excite several Stark states with the first two lasers, yet we observe widths <1 cm^{-1}. Why is there no broadening or additional structure? Previous experiments[18] show that, as expected theoretically, each of the $6snk$ Stark states is only optically connected to the analogous $6pnk$ Stark state, so we only need to consider one Stark state at a time. A particular $6snk \rightarrow 6pnk$ transition is between two nearly identical Stark states which shift up and down in energy together as the microwave field oscillates. Thus there is negligible differential energy shift, and the result is no additional structure or broadening above the intrinsic width of the $6pnk$ level. This notion can be written more formally by writing the $6snk$ and $6pnk'$ Stark-state wave functions in atomic units as[19]

TABLE I. Scaled autoionization rates of Ba $6p_{1/2}nl$ states in atomic units.

l	$n^3\Gamma$
0	0.09[a]
1	0.02[b]
2	0.05[c]
3	0.31[b]
4	0.05[d]
5	0.01[e]
6	0.001[e]
7	0.000 08[e]

[a]See Ref. 14.
[b]See Ref. 16.
[c]See Ref. 15.
[d]See Ref. 17.
[e]See Ref. 4.

$$\psi_{6snk}(r,t)=\psi_{6snk}(r)e^{-iW_{6snk}t}\sum_m J_m\left[\frac{\mu_k E}{\omega}\right]e^{-im\omega t} \quad (4a)$$

and

$$\psi_{6pnk'}(r,t)=\psi_{6pnk'}(r)e^{-iW_{6pnk'}t}\sum_m J_m\left[\frac{\mu_{k'}E}{\omega}\right]e^{-im\omega t}. \quad (4b)$$

Here W_{6snk} are $W_{6pnk'}$ are the energies of the two Stark states in zero field and J_m is a Bessel function, the argument of which depends on the microwave-field amplitude E, the Stark shift of the nk or nk' level, represented by its permanent electric dipole moment μ_k or $\mu_{k'}$, and the microwave angular frequency ω.

In writing Eqs. (4) we have simply replaced the usual single $6snk$ or $6pnk'$ state by a set of sideband states separated by the microwave frequency ω. The number of sideband states depends on the amplitude of the microwave field E, and in the limit $E=0$ only the original $6snk$ and $6pnk'$ states, corresponding to the J_0 Bessel functions, are present. When we calculate the electric dipole matrix element from the $6snk$ sideband states to the $6pnk'$ sideband states it takes the form[19,20]

$$\langle 6pnk'|\mu|6snk\rangle = \langle 6p|\mu|6s\rangle\langle nk'|nk\rangle e^{i(W_{6pnk'}-W_{6snk})t} \times\sum_{mm'} J_m\left[\frac{\mu_{k'}E}{\omega}\right]e^{im\omega t}J_{m'}\left[\frac{\mu_k E}{\omega}\right]e^{-im'\omega t}, \quad (5)$$

where μ is the electric dipole operator. Equivalently, we can rewrite Eq. (5) in the form

$$\langle 6pnk'|\mu|6snk\rangle = \langle 6p|\mu|6s\rangle\langle nk'|nk\rangle \times\sum_l e^{i(W_{6pnk'}-W_{6snk}-l\omega)t} \times\sum_m J_m\left[\frac{\mu_k E}{\omega}\right]J_{m+l}\left[\frac{\mu_{k'}E}{\omega}\right]. \quad (6)$$

Using Bessel function identities Eq. (6) may be rewritten as[21]

$$\langle 6pnk'|\mu|6snk\rangle = \langle 6p|\mu|6s\rangle\langle nk'|nk\rangle \times\sum_l e^{i(W_{6pnk'}-W_{6snk}-l\omega)t} \times J_l\left[\frac{\mu_k-m_{k'})E}{\omega}\right]. \quad (7)$$

The overlap integral $\langle nk'|nk\rangle$ ensures that the right-hand side of Eq. (7) vanishes unless $k'=k$, in which case $\mu_{k'}=\mu_k$ and the argument of the Bessel function is zero. In this case only the $l=0$ Bessel function is nonzero[21] and Eq. (7) collapses to the static field result

$$\langle 6pnk|\mu|6snk\rangle = \langle 6p|\mu|6s\rangle e^{i(W_{6pnk}-W_{6snk})t}. \quad (8)$$

A resonance occurs when the laser angular frequency ω_L matches the $6snk$-$6pnk$ energy. Thus only one line is observed, at the $6snk$-$6pnk$ interval. In other words the effect of the time varying microwave field is the same as that of a static field.

Inspecting Fig. 6 we see that the slope of the plot of autoionization rates versus n^{-4} in microwave fields is slightly smaller than the corresponding plot in dc fields, we attribute at least some of the discrepancy to the scatter in the dc field data. The static field measurements should be much more sensitive to slight changes in Stark state composition with varying field strength since they sample the autoionization rates for single field amplitudes. Microwaves, on the other hand, average out small perturbations in state composition by sampling the contribution to the autoionization rate of numerous Stark states over many microwave cycles. After the excitation of a given Stark state by the second laser pulse, the microwave field makes ~ 100 cycles before the appearance of the third laser pulse. During these cycles, the microwaves act as a mechanism to redistribute the population over many excited Stark states. In addition we attribute the slightly smaller experimental values of the widths in microwave fields to incomplete mixing of the lowest l states with the manifold Stark states, as alluded to above. In any case, the microwave data are in reasonable agreement with the prediction of our simple model.

Forced autoionization in microwave fields

Garton *et al.*[22] observed many years ago the phenomenon which they termed forced autoionization. In zero field a perturbing level in a Rydberg series produces perturbations of the energy levels in direct proportion to the strength of its interaction with the Rydberg series. In the presence of an electric field strong enough to convert the Rydberg states into a continuum the perturbing level is converted into a forced autoionization resonance, the width of which is proportional to the strength of the interseries interaction, as has been verified in detail by subsequent investigations.[23,24] To a reasonable approximation the applied field must be large enough that the Inglis-Teller limit of the Rydberg series lies below the perturbing level. This static field is not sufficient to actually ionize the interacting members of the Rydberg series, but it will convert them into a quasicontinuum.

Here we present an illustration of microwave forced autoionization of the Ba $6p_{3/2}12s_{1/2}$ state which interacts with the Ba $6p_{1/2}ns_{1/2}$ and $6p_{1/2}nd_{3/2}$ series as well as the continua above the $Ba^+6s_{1/2}$ and $5d_j$ limits. To our knowledge this is the first observation of forced autoionization of an already autoionizing state. In Fig. 7 we show the spectra obtained by exciting the bound $6s12s\ ^1S_0$ state to the autoionizing $6p_{3/2}12s_{1/2}$ state in zero field and several microwave fields. As shown in Fig. 7(a), in zero field we observe a broad resonance which is highly structured by the interaction of the broad $6p_{3/2}12s_{1/2}$ state with the $p_{1/2}ns_{1/2}$ and $6p_{1/2}nd_{3/2}$ states. On the low-energy side of the line, 21 800 cm^{-1},

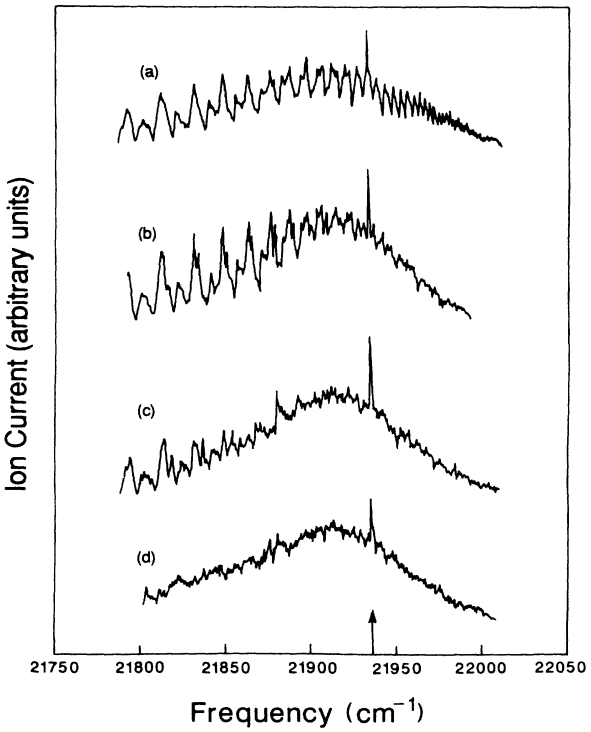

FIG. 7. Third laser frequency scan over the $6p_{3/2}12s$ autoionizing state in the presence of microwave fields. As the microwave power is increased, the interfering $6p_{1/2}ns(d)$ series is gradually converted into a continuum destroying the interference pattern. Measurements were performed in fields of (a) 0 V/cm, (b) 75 V/cm, (c) 260 V/cm, and (d) 875 V/cm. The ionization limit of the $6p_{1/2}$ series in zero field occurs 22 062 cm^{-1}, and the Inglis-Teller limits for (b)–(d) fall at 21 937, 21 857, and 21 727 cm^{-1}, respectively. The sharp feature in all the scans is the $6s6p$-$6s10d$ transition at 21 938 cm^{-1}.

the $6p_{3/2}12s_{1/2}$ state interacts with $6p_{1/2}$ states of $n=20$. At the center of the line, 21 900 cm^{-1}, the interaction is with $6p_{1/2}$ states of $n=26$, and at the 22 000 cm^{-1} the interaction is with $6p_{1/2}$ states of $n=44$. We have used microwave fields of 75, 260, and 875 V/cm, leading to the Inglis-Teller limits 125, 205, and 335 cm^{-1} below the zero-field limit. On the frequency scale of Fig. 7 the Inglis-Teller limits for Figs. 7(b)–7(d) are 21 937, 21 857, and 21 727 cm^{-1}, respectively. As the microwave field is increased more of the structure disappears, as the microwave field converts the $6p_{1/2}$ series into a continuum. In the low field, 75 V/cm, of Fig. 7(b) only high n states above $\sim$21 950 cm^{-1} have diappeared. In Fig. 7(c) the structure is gone above 21 910 cm^{-1}, and in Fig. 7(d) all the structure has disappeared. These observations are in reasonable agreement with the calculated Inglis-Teller limits. In the field of 875 V/cm corresponding to Fig. 7(d), the $6p_{1/2}ns_{1/2}$ and $6p_{1/2}nd_{3/2}$ series are both effectively continua, so the $6p_{3/2}ns_{1/2}$ state is now coupled to continua associated with the $6s_{1/2}$, $5d_j$, and $6p_{1/2}$ limits. Note that the widths of the $6p_{3/2}12s_{1/2}$ resonances (ignoring detailed structure) of Figs. 7(a) and 7(d) are the same. This is a direct demonstration that the zero-field width of the $6p_{3/2}12s_{1/2}$ resonances of Fig. 7(a) is not only from its interaction with the continua above the $6s_{1/2}$ and $5d_j$ limits but also includes a contribution from the interaction with the discrete $6p_{1/2}ns_{1/2}$ and $6p_{1/2}nd_{3/2}$ series.

CONCLUSION

These experiments show rather clearly that the hydrogenic Stark model of Jacobs *et al.*[1,2] gives an excellent description of autionization in both static and dynamic fields, even if the time scale of the field variation is rapid compared to the autoionization or radiative decay rates of the states of interest. The experiments also show very clearly that in fields autoionization rates scale as n^{-4}, not as n^{-3}, as is true in zero field.

Our experiments differ from a real plasma in an important way; the field has a well-defined direction, which means that m remains a good quantum number. In a real plasma the direction of the microfields changes randomly, so that m is not a good quantum number. As a result the autoionization rates of the low l, low m states are mixed not only into the high l states but also into all the m states as well. Therefore, the rapid autoionization rates of the low l states are spread over n^2 states leading to an n^{-5} scaling of the autoionization rates in random microfields. Such an n^{-5} scaling of the autoionization rates would lead to an even greater increase in the dielectronic recombination rate than that produced by a static field.

ACKNOWLEDGMENTS

It is a pleasure to acknowledge useful conversations with D. Hummer and the support of the U.S. Department of Energy, Office of Basic Energy Sciences, Chemical Sciences Division.

[1]V. L. Jacobs, J. Davis, and P. C, Kepple, Phys. Rev. Lett. **37**, 1390 (1976).
[2]V. L. Jacobs and J. Davis, Phys. Rev. A **19**, 776 (1979).
[3]D. A. Park, Z. Phys. **159**, 155 (1960).
[4]R. R. Jones and T. F. Gallagher, Phys. Rev. A **38**, 2846 (1988).
[5]A. L. Merts, R. D. Cowan, and N. H. Magee, Jr., Los Alamos Scientific Laboratory Report No. LA-6200-MS, 1976 (unpublished).
[6]D. S. Belic, G. H. Dunn, T. J. Morgan, D. W. Mueller, and C. Timmer, Phys. Rev. Lett. **50**, 339 (1983).
[7]A. Lindgard and S. E. Nielsen, At. Data Nucl. Data Tables **19**, 534 (1977).
[8]W. E. Cooke, T. F. Gallagher, S. A. Edelstein, and R. M. Hill, Phys. Rev. Lett. **40**, 178 (1976).
[9]N. H. Tran, P. Pillet, R. Kachru, and T. F. Gallagher, Phys. Rev. A **29**, 2640 (1984).
[10]T. W. Hansch, Appl. Opt. **11**, 895 (1972).
[11]U. Eichmann, J. L. Dexter, E. Y. Xu, and T. F. Gallagher, Z. Phys. D (to be published).
[12]W. E. Cooke, S. A. Bhatti, and C. L. Cromer, Opt. Lett. **7**, 69

(1982).
[13]S. M. Jaffe, R. Kachru, N. H. Tran, H. B. van Linden van den Heuvell, and T. F. Gallagher, Phys. Rev. A **30**, 1828 (1984).
[14]W. E. Cooke (private communication).
[15]F. Gounand, T. F. Gallagher, W. Sander, K. A. Safinya, and R. Kachru, Phys. Rev. A **27**, 1925 (1982).
[16]R. R. Jones, C. J. Dai, and T. F. Gallagher (unpublished).
[17]S. M. Jaffe, R. Kachru, H. B. van Linden van den Heuvell, and T. F. Gallagher, Phys. Rev. A **32**, 1480 (1985).
[18]K. A. Safinya, J. F. Delpech, and T. F. Gallagher, Phys. Rev. A **22**, 1062 (1980).
[19]S. H. Autler and C. H. Townes, Phys. Rev. **100**, 703 (1955).
[20]J. H. Shirley, Phys. Rev. **138**, B979 (1965).
[21]*Handbook of Mathematical Functions,* Natl. Bur. Stand. Appl. Math. Ser. No. 55, edited by M. Abramowitz and I. A. Stegun (U.S., GPO, Washington, D.C., 1964).
[22]W. R. S. Garton, W. H. Parkinson, and E. M. Reeves, Proc. Phys. Soc. London **80**, 860 (1962).
[23]W. Sandner, K. A. Safinya, and T. F. Gallagher, Phys. Rev. A **33**, 1008 (1986).
[24]T. F. Gallagher, F. Gounand, R. Kachru, N. H. Tran, and P. Pillet, Phys. Rev. Lett. A **27**, 2485 (1983).